

The coadsorption of nitrogen with carbon monoxide and oxygen on the Ru(001) surface: Local chemical interactions in mixed overlayers

A. B. Anton, N. R. Avery, T. E. Madey, and W. H. Weinberg

Citation: *The Journal of Chemical Physics* **85**, 507 (1986); doi: 10.1063/1.451628

View online: <http://dx.doi.org/10.1063/1.451628>

View Table of Contents: <http://scitation.aip.org/content/aip/journal/jcp/85/1?ver=pdfcov>

Published by the [AIP Publishing](#)

Articles you may be interested in

[Surface diffusion of carbon monoxide and potassium coadsorbed on Ru\(001\): Confirmation of a 1:1 CO:K trapping interaction](#)

J. Chem. Phys. **104**, 7313 (1996); 10.1063/1.471398

[Electronic and chemical interactions between boron and carbon monoxide on Ru\(0001\)](#)

J. Chem. Phys. **96**, 740 (1992); 10.1063/1.462459

[Effects of coadsorbed carbon monoxide on the surface diffusion of hydrogen on Ru\(001\)](#)

J. Chem. Phys. **89**, 5242 (1988); 10.1063/1.455615

[Abstract: Nitrogen, oxygen, and carbon monoxide chemisorption on polycrystalline titanium surfaces](#)

J. Vac. Sci. Technol. **15**, 657 (1978); 10.1116/1.569661

[Coadsorption of Oxygen and Carbon Monoxide upon a \(110\) Tungsten Surface](#)

J. Chem. Phys. **45**, 2383 (1966); 10.1063/1.1727951



The coadsorption of nitrogen with carbon monoxide and oxygen on the Ru(001) surface: Local chemical interactions in mixed overlayers

A. B. Anton,^{a)} N. R. Avery,^{b)} T. E. Madey,^{c)} and W. H. Weinberg

Division of Chemistry and Chemical Engineering, California Institute of Technology, Pasadena, California 91125

(Received 28 February 1986; accepted 20 March 1986)

High resolution electron energy loss spectroscopy and thermal desorption mass spectrometry have been employed to investigate the molecular chemisorption of N₂ on both disordered and ordered overlayers of atomic oxygen on the Ru(001) surface, as well as the chemisorption of CO on overlayers of N₂ on Ru(001). Pertinent results obtained for the adsorption of N₂ on the clean Ru(001) surface are also presented for comparison. *Disordered* oxygen poisons a fraction of the surface to the subsequent adsorption of N₂ whereas the N₂ that does adsorb is indistinguishable from N₂ on clean Ru(001). The fraction of the surface that is poisoned to the adsorption of N₂ is approximately twice the fractional surface coverage of disordered oxygen. The $p(2 \times 2)$ overlayer of *ordered* oxygen adatoms, which is formed at a fractional surface coverage of 0.25, stabilizes the chemisorption of N₂ into a new binding state with a heat of adsorption that is approximately 1.5 kcal/mol greater than any one observed for the adsorption of N₂ on the clean surface. Coverage measurements indicate that this state results from the stoichiometric addition of one N₂ molecule to each unit cell of the $p(2 \times 2)$ -O overlayer. Electron energy loss spectroscopic results suggest that this N₂ binding state results from stabilization of the dominant σ donor contribution to the Ru-N₂ bond, due to the presence of the electronegative oxygen adatoms of the $p(2 \times 2)$ overlayer. Measurements of the adsorption of CO on saturated overlayers of N₂ show that N₂ is displaced from the surface by increasing coverages of subsequently adsorbed CO. For low coverages of CO in the presence of N₂, the observed value of $\nu(\text{CO})$ is lower than observed under any conditions for the adsorption of CO alone on the Ru(001) surface. The N₂ ad molecules enhance the ability of the surface ruthenium atoms to backdonate electron density into the 2π orbital of coadsorbed CO under these conditions. At coverages of CO in excess of 0.10 monolayer, the results are consistent with CO island formation and segregation of N₂ and CO ad molecules into different local regions on the surface.

I. INTRODUCTION

Traditionally, CO has served as the prototypical adsorbate for molecular chemisorption studies on single crystal-line metal surfaces. Theoretical calculations of the electronic structure of chemisorbed CO¹⁻³ have provided both a thorough understanding of the nature of the metal-CO bond and a detailed interpretation of the results of photoemission experiments. Investigations of the chemisorption of CO on metals employing vibrational spectroscopy have made use of the σ donation and π^* backdonation interpretation of metal-CO bonding provided by these calculations to correlate CO stretching frequencies both with the adsorption site geometry (e.g., on-top, twofold bridge, etc.)⁴ and with coverage-dependent changes in the metal-CO bond.^{3,5} Furthermore, chemisorbed overlayers of CO have served as model systems for theoretical investigations which treat adsorbed molecules as oscillating point dipoles in order to calculate inelastic scattering cross sections and describe coverage-dependent frequency shifts.^{4,6}

Since N₂ is isoelectronic with and structurally similar to CO, the investigation of the chemisorption of N₂ and a comparison to CO is the logical next step in understanding better both surface chemical bonding and interactions among adsorbed molecules. Recognizing this, there have been a number of recent theoretical⁷⁻¹⁰ and experimental¹¹⁻¹³ investigations that compare the bonding of N₂ and CO to metals, and from these studies a clear picture of the differences between metal-N₂ and metal-CO bonding has evolved.¹⁴ Briefly, bonding of both CO and N₂ to a metal surface occurs via a combination of σ electron donation from CO or N₂ to the metal and backdonation from the metal conduction band to the otherwise unoccupied antibonding π^* orbitals of CO or N₂. For CO, the σ donor bond results from the interaction of the 5σ "lone pair" orbital of CO, localized on the carbon atom, with the conduction band of the metal surface. For N₂, however, the σ valence orbitals, $2\sigma_u$ and $3\sigma_g$, are shared equally between the two nitrogen atoms in the free molecule, and although they mix upon interaction with a metal surface to form two new σ orbitals with some lone pair character; the resulting donor bond is weaker, in general, than that of CO. Backdonation from the conduction band of the metal to the 2π antibonding level of CO weakens the C \equiv O bond and lowers $\nu(\text{CO})$ from its gas phase value upon adsorption. Analogous arguments apply to the $1\pi_g$ antibonding orbital of N₂, and changes in the extent of backdonation with sur-

^{a)} Current address: Chemical Engineering Department, Cornell University, Ithaca, New York 14853.

^{b)} Current address: Division of Materials Science, C.S.I.R.O., Normandy Rd., Locked Bag 33, Clayton, Victoria, Australia.

^{c)} Current address: Surface Chemistry Section, Institute for Materials Research, National Bureau of Standards, Washington, D.C. 20234.

face coverage can cause both $\nu(\text{CO})$ and $\nu(\text{NN})$ to vary with coverage. However, back donation is expected to be more important in the case of CO than N_2 , since the 2π orbital of CO lies at a lower energy than the corresponding $1\pi_g$ orbital of N_2 .¹⁵ Finally, $\nu(\text{CO})$ and $\nu(\text{NN})$ can be affected by the presence of coadsorbed species which either suppress¹⁶ or enhance¹⁷ back donation.

This paper presents the results of an experimental investigation which applies high resolution electron energy loss vibrational spectroscopy (EELS) and thermal desorption mass spectrometry (TDMS) to the identification of the structure and bonding of the adsorbed species present in mixed overlayers of atomic oxygen and N_2 , and of CO and N_2 on the Ru(001) surface. The aim of this investigation is to understand more quantitatively the appropriateness of the bonding ideas outlined above. Oxygen coadsorption with N_2 was chosen to investigate the effects of an increase in the "Lewis acidity" of the surface metal atoms on the bonding of N_2 to the surface, and to compare the results to those of previous investigations of oxygen and CO coadsorption on Ru(001).^{18,19} Carbon monoxide coadsorption with N_2 was chosen to investigate intermolecular interactions (including those mediated by the ruthenium substrate) between adsorbed CO and N_2 molecules, with particular emphasis on the effects manifest in the vibrational spectra of each species. For completeness and comparison, results obtained for the adsorption of N_2 on the clean Ru(001) surface are also presented and are discussed more fully than heretofore.²⁰

II. EXPERIMENTAL PROCEDURES

The measurements described here were performed in a stainless steel, ion pumped ultrahigh vacuum system with a base pressure below 1×10^{-10} Torr. Its description, including details pertinent to the EELS and TDMS experiments, is presented in Ref. 21, and the preparation of the Ru(001) sample is documented in Ref. 18.

The crystal was exposed to the gases by backfilling the vacuum chamber through leak valves. The CO, O_2 , and $^{14}\text{N}_2$ gases were Matheson Research Purity (99.9% minimum), and the $^{15}\text{N}_2$ was obtained from Prochem (99 at. % ^{15}N). Exposures are reported in units of Langmuirs ($1 \text{ L} \equiv 1 \text{ Langmuir} \equiv 10^{-6} \text{ Torr s}$), measured with a Bayard-Alpert ionization gauge and uncorrected for relative ionization cross sections.

Adsorption temperatures of 75 K were reached by pumping on the cooling reservoir of the crystal manipulator with a mechanical vacuum pump, while feeding liquid nitrogen at atmospheric pressure to the reservoir through a restriction orifice. This allowed continuous operation of the reservoir at a total pressure near 160 Torr, where the boiling temperature of nitrogen is approximately 65 K. Crystal temperatures were measured with a calibrated W-26%Re/W-5%Re thermocouple, which was spot welded to the rear face of the single crystal.

The crystal was cleaned by repeated thermal cycling between 400 and 1100 K in 5×10^{-8} Torr of O_2 to oxidize surface impurities, followed by annealing to 1750 K to remove all chemisorbed oxygen. Occasional Ar^+ bombardment was also used to clean the surface. Surface cleanliness

was monitored via EELS and thermal desorption spectra, and the surface was judged clean when the EEL spectrum was featureless, and the peak positions and intensities in thermal desorption spectra for various coverages of CO were reproduced.

The EEL spectra were collected in the specular direction with a resolution of $70\text{--}80 \text{ cm}^{-1}$ (full width at half-maximum), while maintaining an electron count rate of 1 to 3×10^5 cps in the elastically scattered beam. Peak positions in the EEL spectra are accurate to approximately $\pm 5 \text{ cm}^{-1}$, based on numerous measurements under ostensibly the same conditions. The electron beam was incident on the crystal at 60° from the surface normal, and the kinetic energy of the incident electron beam at the surface varied between 4 and 5 eV, unless otherwise noted.

Thermal desorption measurements were conducted in a line-of-sight configuration with a UTI 100C quadrupole mass spectrometer, oriented approximately 40° from the sample normal and controlled by a DEC PDP 11/10 laboratory computer. This system allowed multiplexing for simultaneous collection of thermal desorption spectra at several m/e ratios and provided routines for accurate determinations of peak areas for surface coverage measurements. Surface coverages for the N_2 thermal desorption spectra were obtained by comparison of the integrated areas of the desorption traces to those obtained for desorption from a saturated monolayer of CO on the Ru(001) surface of which the latter represents a fractional coverage of 0.65.²² Coverages obtained by this method are reproducible and precise to $\pm 5\%$, but a potential systematic error resulting from the calibration against the desorption of CO makes their accuracy uncertain by an estimated $\pm 15\%$. The surface coverages obtained for the thermal desorption spectra of N_2 by this method, however, do show excellent agreement (approximately 10% discrepancy) with those reported in Ref. 23, where coverages for N_2 on Ru(001) were calibrated against the desorption of N_2 from a $(\sqrt{3} \times \sqrt{3})\text{R}30^\circ$ ordered overlayer, the fractional surface coverage of which is 0.33. Oxygen coverages were obtained by first identifying the O_2 exposures necessary to form the $p(2 \times 2)$ ($\theta = 0.25$) and the $p(1 \times 2)$ ($\theta = 0.50$) ordered overlayers of atomic oxygen on Ru(001),²⁴ and then using these known exposures to scale the exposure versus surface coverage data given for the adsorption of O_2 on Ru(001) in Ref. 25. The surface coverages of atomic oxygen obtained by this method are accurate to an estimated $\pm 15\%$.

III. RESULTS AND DISCUSSION

A. The adsorption of nitrogen on the clean Ru(001) surface

Exposure of the clean Ru(001) surface at 95 K to N_2 produces a single first-order thermal desorption peak, the temperature of which shifts from 128 K at low coverage to 119 K at saturation coverage. The binding energy of this state, estimated for first-order desorption kinetics and neglecting interadsorbate interactions,²⁶ is approximately 7.2 kcal/mol.²⁷ The saturation fractional coverage of N_2 adsorbed at 95 K, estimated via comparison to the desorption of known coverages of CO, is 0.35. This is consistent with the

observation of a $(\sqrt{3} \times \sqrt{3})R30^\circ$ low-energy electron diffraction (LEED) pattern under these experimental conditions.^{23,29}

The EEL spectra recorded after adsorption at 95 K show two dipolar-enhanced modes. The frustrated translation of the N_2 molecules perpendicular to the surface, $\nu(\text{Ru-N}_2)$, appears initially at 280 cm^{-1} and shifts with increasing coverage to 298 cm^{-1} at saturation; while the nitrogen-nitrogen stretching vibration, $\nu(\text{NN})$, appears initially at 2252 cm^{-1} and shifts to 2212 cm^{-1} at saturation. By analogy to the vibrational spectra of linear Ru-N_2 inorganic compounds, which show $\nu(\text{NN})$ between 2085 and 2125 cm^{-1} ,³⁰ these results suggest strongly that the N_2 molecules are coordinated to the surface at on-top sites, and the absence of bending modes in the spectra indicates that their interatomic axes are essentially perpendicular to the surface.

Of particular interest is the decrease in $\nu(\text{NN})$ of 40 cm^{-1} which is observed between very low and saturation coverage at this temperature of adsorption. A well-established theory describing the interaction of electrons with arrays of oriented dipoles^{4,6} shows that the same physical properties of an adsorbed overlayer which cause inelastic scattering of electrons via a dipolar interaction also produce vibrational coupling among the molecules of the adsorbed overlayer, and that this dipolar coupling causes vibrational frequencies to increase monotonically with increasing surface coverage. Subtraction of this contribution of approximately 12 cm^{-1} (see the Appendix) from the total shift in $\nu(\text{NN})$ with increasing surface coverage indicates that the actual decrease in $\nu(\text{NN})$ due to coverage-dependent changes in the $\text{N}\equiv\text{N}$ bond is approximately 52 cm^{-1} .

Although negative frequency shifts with increasing surface coverage have been reported for the $\nu(\text{CO})$ mode of CO adsorbed on both $\text{Cu}(111)$ ³¹ and on polycrystalline gold³² and for the $\nu(\text{NN})$ mode of N_2 adsorbed on $\text{Ni}(110)$,³³ these observed decreases in $\nu(\text{CO})$ and $\nu(\text{NN})$ were less than 10 cm^{-1} , and no detailed explanations for the change in the $\text{C}\equiv\text{O}$ or $\text{N}\equiv\text{N}$ bond with increasing surface coverage were offered. One possible explanation for this effect attributes the decrease in $\nu(\text{NN})$ with increasing coverage to the formation of a $1\pi_g$ band, broadening the energy of this π^* antibonding level and causing its population to vary due to coverage-dependent changes in its overlap with the occupied conduction band of the metal substrate. This mechanism was first offered to explain the results of infrared reflection absorption spectroscopic measurements of mixed overlayers of ^{12}CO and ^{13}CO on $\text{Cu}(110)$, where chemical interactions among adsorbed CO molecules were identified which produce a downward shift of $\nu(\text{CO})$ with increasing surface coverage, more than compensating for the upward shift due to dipolar coupling.³⁴ More recent UV photoemission³⁵ and Bremsstrahlung isochromat spectroscopic³⁶ results have identified dispersion in the 2π band of adsorbed CO, providing at least indirect support for this interpretation for the particular case of CO adsorbed on copper surfaces.

The arguments presented in Ref. 34 for CO on $\text{Cu}(110)$ can be readily cast in terms appropriate to the phenomena observed for the adsorption of N_2 on $\text{Ru}(001)$. Since the energy of the $1\pi_g$ orbital of an isolated, chemisorbed N_2

molecule on the $\text{Ru}(001)$ surface lies above the Fermi level, the $1\pi_g$ orbital is unpopulated and does not affect $\nu(\text{NN})$. Increasing the density of N_2 ad molecules on the surface, however, could cause the $1\pi_g$ orbitals of neighboring molecules to overlap and interact, and at sufficiently high coverages, a band with significant energy dispersion would result. Band formation even at coverages of N_2 below $\theta = 0.33$ is possible since the spatial extent of the $1\pi_g$ orbital of N_2 is greater than its van der Waals diameter (approximately 5.6 \AA), allowing significant overlap at the intermolecular spacing of 4.66 \AA which obtains for the $(\sqrt{3} \times \sqrt{3})R30^\circ$ unit cell. Island formation at low coverage, as is observed experimentally for CO on $\text{Ru}(001)$ ³⁷ and in simulations for N_2 on $\text{Ru}(001)$ ²⁸ would enhance this effect. If the $1\pi_g$ band broadens sufficiently with increasing coverage to cross the Fermi level, increasing the population of this band by increasing the coverage would cause the $\text{N}\equiv\text{N}$ bond to weaken and $\nu(\text{NN})$ to decrease. However, this mechanism does not take into account a possible perturbation of the electronic structure of the metal substrate by the adsorbed overlayer. This issue will be considered in more detail in conjunction with results obtained for the coadsorption of N_2 and CO on the $\text{Ru}(001)$ surface, presented in Sec. III C.

Results of thermal desorption measurements after the adsorption of N_2 on the clean $\text{Ru}(001)$ surface at 75 K are shown in Fig. 1. Initial exposure produces the state near 125 K, as was described for adsorption at 95 K. For exposures of 1.0 L or greater ($\theta \geq 0.22$), however, a second feature appears near 105 K, which shifts continuously to 90 K for a saturation exposure of 2.5 L or greater. The saturation coverage of N_2 observed under these conditions is approximately 0.5 monolayer. The results of LEED measurements show the development of a weak, diffuse $(\sqrt{3} \times \sqrt{3})R30^\circ$ pattern indicating the presence of substantial disorder in the overlayer upon adsorption at 75 K.²³ This disorder is manifest as

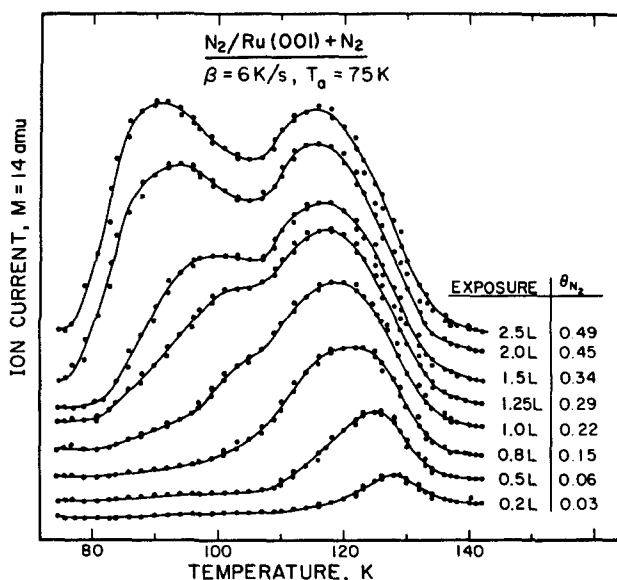


FIG. 1. Thermal desorption spectra of N_2 ($m = 14\text{ amu}$) recorded after the indicated exposures of the clean $\text{Ru}(001)$ surface to N_2 at 75 K. The fractional surface coverages of N_2 for each exposure are also listed. The heating rate β for these measurements is 6 K/s .

a larger number of smaller islands at low coverages, a larger number of out-of-phase domain boundaries at fractional coverages near 0.33, and the overlap of out-of-phase domains at higher coverages.²⁸ The probability of adsorption triples from its initial value of approximately 0.25 when the low temperature state begins to populate.^{23,28} As demonstrated in Fig. 2, thermal desorption spectra recorded after a 2.0 L exposure of the Ru(001) surface to $^{15}\text{N}_2$ at 100 K to populate the high temperature state, followed by a 2.0 L exposure of the surface to $^{14}\text{N}_2$ at 75 K (or vice versa), show *incomplete mixing* of the two isotopes upon desorption. This precludes the possibility of simple two-dimensional compression of the overlayer at high coverage as occurs, for example, for CO adsorption on Ru(001).²² Indeed, this low temperature thermal desorption state is due entirely to repulsive interactions among the N_2 ad molecules, as opposed, for example, to the occupation of geometrically different binding sites on the surface.²⁸

Figure 3 illustrates the effects of the adsorption temperature on the relative populations of the two binding states. The thermal desorption spectrum recorded after a saturation exposure of the Ru(001) surface to N_2 at 75 K (Fig. 3, *top*, $\theta = 0.50$) shows decreased population of the high temperature state relative to the spectrum obtained for a saturation exposure at 95 K (Fig. 3, *middle*, $\theta = 0.35$), indicating nonequilibrium adsorption at 75 K, with population of the low temperature state occurring at the expense of population in the high temperature state. From the decrease in the intensity of the high temperature state after adsorption at 95 K compared to 75 K, it can be concluded that the surface density (N_2 molecules/Ru surface atom) in the low temperature state is twice to three times that of the high temperature state, where each N_2 ad molecule is associated with three ruthenium surface atoms ($\theta \approx 0.33$). As shown in

the thermal desorption spectrum at the bottom of Fig. 3 ($\theta = 0.46$), the high temperature state, when saturated, poisons the surface significantly for subsequent adsorption into the low temperature state, due to the presence of fewer but larger $\sqrt{3}$ domains after adsorption at 95 K.

Although the thermal desorption results show two *apparent* binding states for N_2 on Ru(001) at 75 K, EEL spectra recorded after adsorption at 75 K, illustrated in Fig. 4, show only two modes, $\nu(\text{Ru}-\text{N}_2)$ and $\nu(\text{NN})$, as were observed after adsorption at 95 K. Furthermore, the coverage dependence of the frequencies of these modes, shown in Fig. 5, is similar to that observed for adsorption at 95 K, i.e., $\nu(\text{NN})$ shifts downward from 2247 to 2198 cm^{-1} at saturation, and $\nu(\text{Ru}-\text{N}_2)$ shifts upward from 278 to 291 cm^{-1} (cf. 2252 to 2212 cm^{-1} and 280 to 298 cm^{-1} for adsorption at 95 K). Finally, the intensities of these bands increase monotonically with increasing surface coverage of both apparent binding states, as may be seen in Fig. 6, exceeding the intensities of $\nu(\text{Ru}-\text{N}_2)$ and $\nu(\text{NN})$ that are observed for saturation coverage at 95 K by 20% and 50%, respectively. Measurements of the intensities of these bands as a function of N_2 surface coverage were also made with an incident electron beam energy of approximately 6.5 eV to insure that possible resonance scattering effects⁴ were not contributing

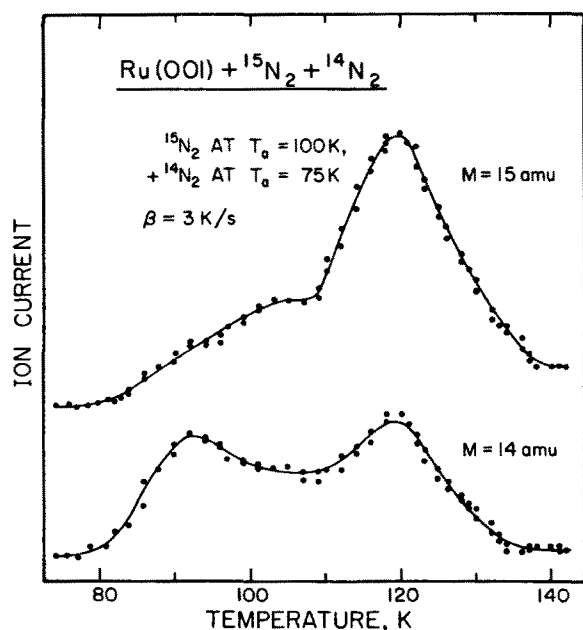


FIG. 2. Thermal desorption spectra of $^{15}\text{N}_2$ ($m = 15$ amu) and $^{14}\text{N}_2$ ($m = 14$ amu) collected simultaneously after exposures of the clean Ru(001) surface first to 2 L $^{15}\text{N}_2$ at 100 K, and then to 2 L $^{14}\text{N}_2$ at 75 K.

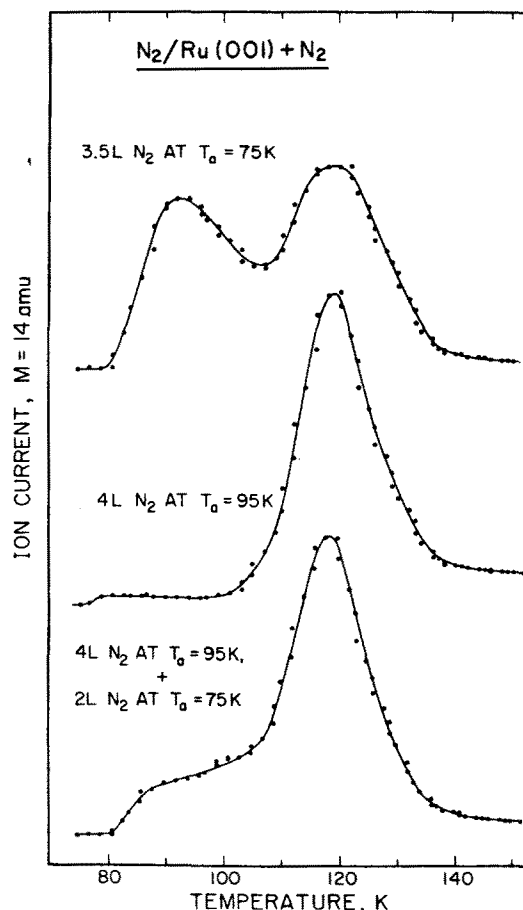


FIG. 3. Thermal desorption spectra of N_2 following the indicated exposures of the clean Ru(001) surface to N_2 at the indicated temperatures, illustrating the effects of the adsorption temperature on the relative populations of the two binding states for N_2 .

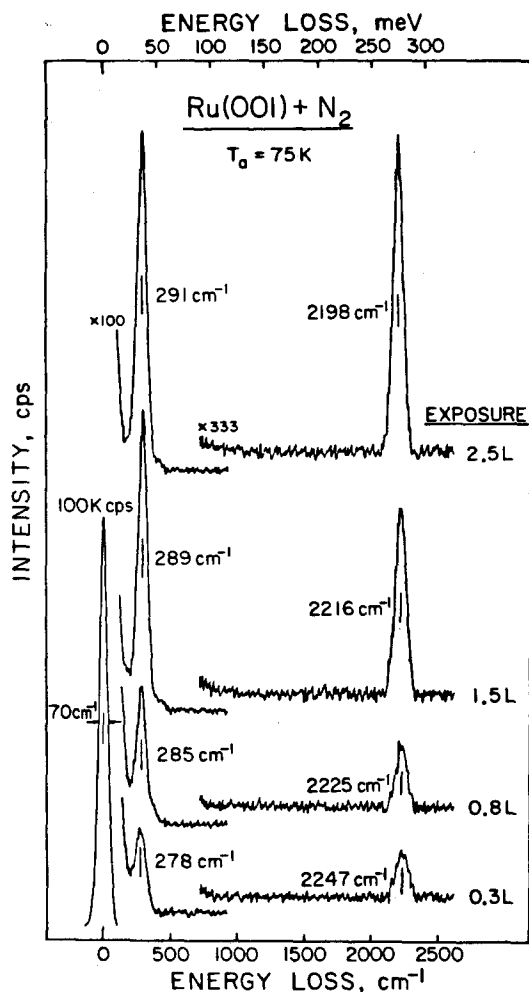


FIG. 4. EEL spectra recorded following the indicated exposures of the Ru(001) surface to N_2 at 75 K.

to the observations, and results quantitatively identical to those shown for a beam of energy of 4 eV were obtained.

The addition of the second apparent binding state of N_2 , present only for adsorption at 75 K, contributes no additional vibrational features to the specular EEL spectrum, causes no additional features to appear in off-specular EELS measurements, causes no abrupt changes in the electron reflectivity of the ruthenium surface, and causes no detectable increase in the linewidth of either EELS band. This, coupled with the monotonic increase in the intensities of both EELS bands with increasing surface coverage of both binding states, indicates that the EELS results are probing the vibrational structure of both chemisorbed states, i.e., the vibrational spectra of the two states are identical within the resolution of the EELS measurements. Consequently, it can be concluded that the N_2 molecules in the low temperature state are also bonded to the ruthenium surface atoms at on-top sites with their molecular axes perpendicular to the surface plane. However, as was illustrated by the thermal desorption results of Fig. 3, which showed that the surface density in the low temperature state is twice to three times that of the high temperature state, the N_2 molecules in the low temperature state are bonded in areas that are locally "crowded" with N_2 admolecules. These molecules desorb at

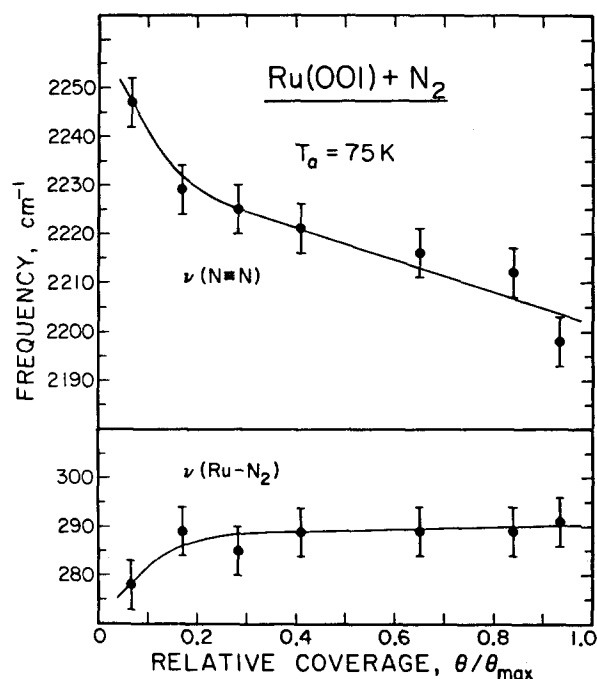


FIG. 5. Vibrational frequencies of adsorbed N_2 as a function of relative surface coverage for adsorption on the Ru(001) surface at 75 K. The saturation coverage of N_2 under these conditions θ_{\max} is approximately 0.5 monolayer.

a lower temperature due to repulsive lateral interactions in the overlayer.²⁸

All of these experimental results can be described by the following scenario. Upon adsorption at 95 K, the N_2 molecules prefer to bind in more favorable adsorption sites, and attractive next-nearest neighbor lateral interactions at the $(\sqrt{3} \times \sqrt{3})R30^\circ$ intermolecular distance on the Ru(001) surface (4.66 Å) lead to the formation of rather large domains of $(\sqrt{3} \times \sqrt{3})R30^\circ$ periodicity. Upon adsorption at 75 K, however, a larger number of smaller islands of the $(\sqrt{3} \times \sqrt{3})R30^\circ$ structure form until the fractional surface coverage approaches 0.2. Subsequent adsorption of N_2 not

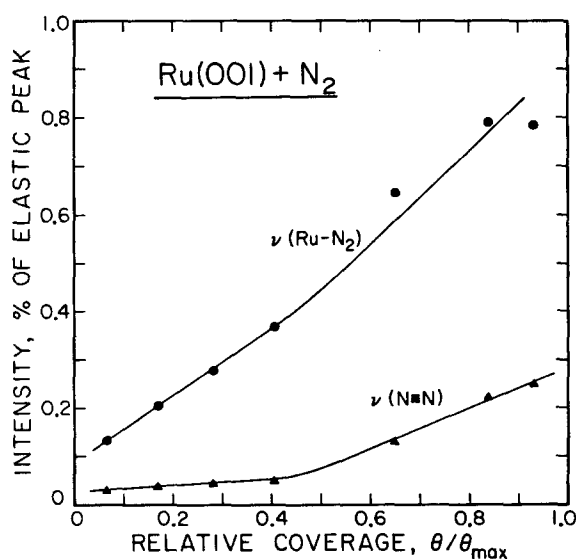


FIG. 6. Intensities of the EELS bands of adsorbed N_2 as a function of relative surface coverage for adsorption on the Ru(001) surface at 75 K.

only contributes to the development of the high temperature state associated with the $(\sqrt{3} \times \sqrt{3})R30^\circ$ superstructure, but also results in N_2 molecules both adsorbed at antiphase domain boundaries between the three independent $\sqrt{3}$ domains and adsorbed within overlapping $\sqrt{3}$ domains where the resulting intermolecular spacing is less than the $\sqrt{3}$ distance. The latter results in a net repulsive intermolecular interaction which decreases the effective binding energy of the N_2 to the surface. The last molecules to adsorb on the surface before saturation coverage is reached are most likely to be bound in these less favorable adsorption sites and are therefore most likely to desorb in the low temperature peak associated with repulsive lateral interactions. However, a fraction of the molecules adsorbed in the $(\sqrt{3} \times \sqrt{3})R30^\circ$ superstructure at low surface coverage must desorb in the low temperature peak due to repulsive interactions with the N_2 molecules added at high coverage. As molecules desorb from the saturated overlayer, they leave adjacent molecules in the $(\sqrt{3} \times \sqrt{3})R30^\circ$ structure, free of repulsive lateral interactions, to desorb in the high temperature peak. Furthermore, some molecules which are *adsorbed* in unfavorable sites at high surface coverage will be relieved of repulsive lateral interactions during desorption and will *desorb* in the high temperature peak. This explains the *partial* mixing of $^{14}N_2$ and $^{15}N_2$ in the desorption spectra of Fig. 2. All aspects of this scenario for adsorption, surface ordering and desorption, including the coverage dependence of the probability of adsorption, are *quantitatively* duplicated in a recent Monte Carlo simulation of this system.²⁸ The results of these calculations indicate that the binding energy of N_2 on Ru(001) in the limit of zero coverage is 5.8 kcal/mol, that attractive next-nearest neighbor lateral interactions of 0.45 kcal/mol exist at the $(\sqrt{3} \times \sqrt{3})R30^\circ$ intermolecular spacing of 4.66 Å, and that repulsive lateral interactions of 0.25 kcal/mol exist at the Ru–Ru (near-neighbor) spacing of 2.70 Å. Consequently, the states of adsorbed N_2 that are observed in the thermal desorption spectra are due entirely to intermolecular interactions. The local binding site, on-top of a ruthenium surface atom, is in all cases the same.

B. The adsorption of nitrogen on Ru(001) surfaces precovered with both disordered and ordered overlayers of oxygen adatoms

Exposure of the clean Ru(001) surface to O_2 at 100 K results in the formation of disordered overlayers of atomic oxygen, the properties of which have been characterized previously employing EELS,²⁴ and LEED, TDMS, and contact potential difference ($\Delta\phi$) measurements.²⁵ The oxygen adatoms occupy threefold hollow sites on the surface, and the saturation fractional coverage of atomic oxygen is approximately 0.5 monolayer.

Thermal desorption spectra of N_2 recorded after varying exposures of the Ru(001) surface to O_2 at 100 K, followed by exposure to N_2 at 75 K (*not shown*), indicate that the primary effect of *disordered* oxygen is to poison a fraction of the surface to subsequent N_2 adsorption, leaving the remainder of the surface to bind N_2 into states indistinguishable from those observed on the clean surface. The peak

shapes and relative intensities of these thermal desorption spectra are very similar to those observed for the adsorption of N_2 on the clean Ru(001) surface (cf. Fig. 1), but the intensities of both peaks are attenuated proportionally to the precoverage of disordered atomic oxygen. This suggests the presence of repulsive short-range interactions between N_2 ad molecules and disordered oxygen adatoms.

For fractional surface coverages of disordered atomic oxygen below 0.25, annealing the surface to temperatures in excess of 300 K causes the oxygen adatoms to *order* into a $p(2 \times 2)$ superstructure, which reaches full development at $\theta = 0.25$.^{24,25} For fractional surface coverages between 0.25 and 0.50, the oxygen adatoms occupy threefold sites within those of the $p(2 \times 2)$ overlayer,²⁴ producing three independent domains of a $p(1 \times 2)$ superstructure, rotated 120° with respect to each other. The saturation coverage of ordered oxygen is 0.5 monolayer, consistent with the presence of the $p(1 \times 2)$ domains.

Thermal desorption spectra of N_2 recorded after the preparation of ordered overlayers of atomic oxygen with varying fractional surface coverages, followed by exposure to 1.5 L of N_2 at 75 K, are shown in Fig. 7. For comparison, the top spectrum shows desorption of N_2 after the same exposure of the clean surface to N_2 . As the surface coverage of ordered oxygen is increased from zero to 0.25, the desorption states of N_2 associated with the clean surface at 94 and 117 K attenuate, and a new feature appears at 140 K. For fractional surface coverages of ordered oxygen adatoms between 0.25 and 0.50, the clean surface states are nearly extinguished, and the state at 140 K is attenuated. For a saturation coverage of ordered oxygen of 0.50 monolayer, almost no adsorption of N_2 is observed. The weak desorption peak near 90 K for coverages of ordered oxygen in excess of 0.25 monolayer is associated either with imperfections in the crystal surface, with imperfections in the order of the atomic oxygen overlayers, or with desorption from the crystal edges or support leads, and is not associated with the well-ordered regions of the crystal surface from which the majority of the

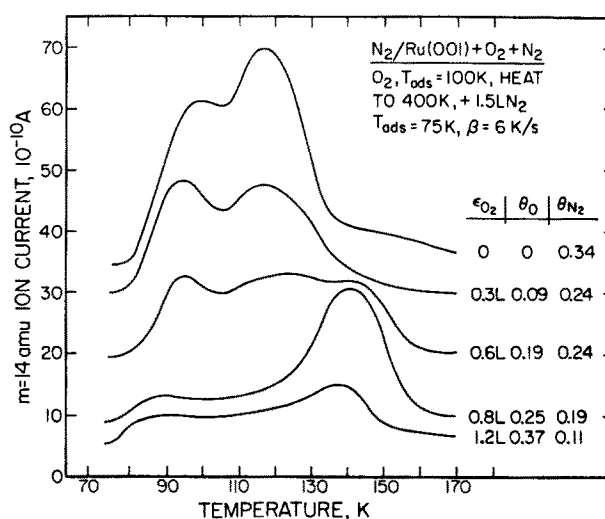


FIG. 7. Thermal desorption spectra of N_2 ($m = 14$ amu) recorded after exposure of the Ru(001) surface, precovered with the indicated fractional surface coverages of ordered oxygen adatoms, to N_2 at 75 K.

desorption of N_2 originates. This assertion has been verified with EELS, which shows no loss peaks due to adsorbed N_2 after exposure of the Ru(001) surface, precovered with the fully developed $p(1 \times 2)$ overlayer of atomic oxygen, to N_2 at 75 K, conditions under which only the (weak) feature at 90 K is observed in TDMS. Thermal desorption spectra are shown in Fig. 8, which were recorded after increasing exposures of the Ru(001) surface upon which a $p(2 \times 2)$ ordered overlayer of oxygen adatoms is present, to N_2 at 75 K. The N_2 state which is stabilized by the presence of the oxygen adatoms of the $p(2 \times 2)$ overlayer first appears at 149 K (the corresponding binding energy is approximately 8.7 kcal/mol²⁶) and shifts to 141 K (8.3 kcal/mol) with increasing coverage. The saturation fractional coverage of N_2 attainable under these conditions depends critically on the fractional surface coverage of oxygen present on the surface prior to the exposure to N_2 . Values between 0.21 and 0.26 for the fractional surface coverage of N_2 were observed, and these results, compared with the ideal fractional surface coverage of the $p(2 \times 2)$ overlayer of oxygen of 0.25, indicate that one N_2 molecule is adsorbed within each unit cell of the $p(2 \times 2)$ overlayer.

A comparison of the vibrational spectra of N_2 adsorbed on both disordered and ordered overlayers of oxygen is presented in Fig. 9. The EEL spectrum recorded after exposure of the clean Ru(001) surface to 0.8 L of O_2 at 100 K (upper left panel), an exposure sufficient to produce a quarter-monolayer of disordered oxygen adatoms, shows the $\nu(\text{RuO})$ mode at 558 cm^{-1} and a shoulder at 427 cm^{-1} which results from disorder present in the oxygen overlayer under these conditions.²⁴ Subsequent exposure of the surface to 2 L of N_2 at 75 K gives a fractional surface coverage of N_2 of 0.16 monolayer and produces the EEL spectrum shown in the upper right panel of Fig. 9. The vibrations due to adsorbed N_2 appear at 268 and 2232 cm^{-1} , differing by only 20 and 8 cm^{-1} from their expected values for the same coverage of N_2 on the clean surface (288 and 2224 cm^{-1} , respectively; cf. Fig. 5). Moreover, the ratio of the intensity of $\nu(\text{Ru-N}_2)$ to that of $\nu(\text{NN})$ is approximately 3:1, as was observed on the clean surface. This suggests that the N_2 molecules adsorbed in the presence of disordered atomic oxygen on Ru(001) are

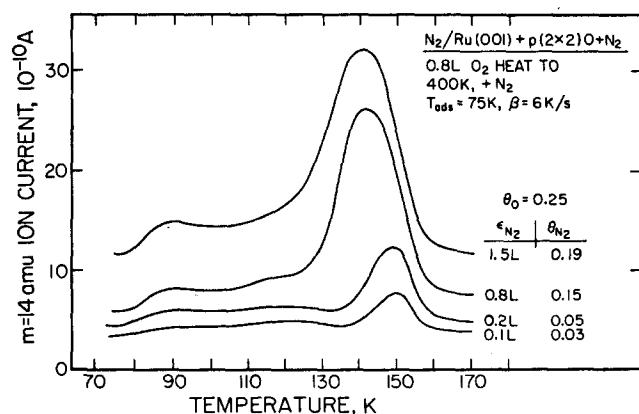


FIG. 8. Thermal desorption spectra of N_2 recorded after the indicated exposures of N_2 at 75 K to the Ru(001) surface on which a $p(2 \times 2)$ overlayer of oxygen adatoms is present.

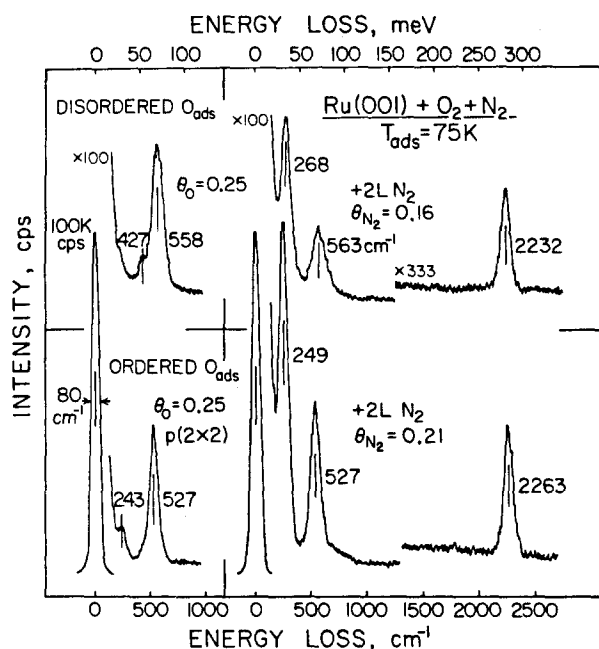


FIG. 9. EEL spectra comparing the vibrational structure of a disordered quarter-monolayer of oxygen adatoms (upper left panel), followed by exposure to 2 L N_2 at 75 K (upper right panel), to that of a $p(2 \times 2)$ ordered quarter-monolayer of oxygen adatoms (lower left panel), followed by exposure to 2 L N_2 at 75 K (lower right panel).

bonded in identical sites with a very similar local environment to those available on the clean surface, in agreement with the results of the TDMS measurements described earlier.

The EEL spectrum in the lower left panel of Fig. 9 shows the effects of annealing to 400 K the surface on which the disordered quarter-monolayer of atomic oxygen is present. The $\nu(\text{RuO})$ feature sharpens and shifts to 527 cm^{-1} , the shoulder at 427 cm^{-1} disappears, and a weak mode due to coupling of the $p(2 \times 2)$ overlayer to a surface phonon appears at 243 cm^{-1} .²⁴ Subsequent exposure to 2 L of N_2 at 75 K gives a fractional surface coverage of N_2 of 0.21 and produces the EEL spectrum shown in the lower right panel of Fig. 9. Note that the ratio of the intensity of $\nu(\text{Ru-N}_2)$ to that of $\nu(\text{NN})$ is now approximately 6:1. Furthermore, $\nu(\text{Ru-N}_2)$ appears at 249 cm^{-1} , 30 cm^{-1} lower than the lowest value observed for adsorption on the clean surface, and $\nu(\text{NN})$ appears at 2263 cm^{-1} , 15 cm^{-1} higher than the highest value observed on the clean surface and 43 cm^{-1} higher than observed for the same fractional coverage of N_2 on the clean surface (cf. Fig. 5). Thus the vibrational spectrum of the binding state produced by the interaction of adsorbed N_2 with the $p(2 \times 2)$ oxygen overlayer is significantly different from that of the N_2 which exists on either the clean Ru(001) surface or in the presence of disordered oxygen. Despite these differences, however, the high frequency of $\nu(\text{NN})$ observed in this spectrum confirms that coordination of N_2 to on-top sites, as observed for adsorption on the clean surface, also obtains in the presence of the $p(2 \times 2)$ overlayer of oxygen.

The effects of the $p(2 \times 2)$ oxygen overlayer on subsequently adsorbed N_2 manifest both in the thermal desorption and EELS results, can be quantitatively understood by

considering the chemical effect on the properties of the Ru(001) surface. Measurement of the contact potential difference between the clean Ru(001) surface and the surface prepared with the $p(2 \times 2)$ oxygen overlayer gives $\Delta\phi = 0.20$ eV.²⁵ Ignoring polarization effects and utilizing a Ru=O bond length of 2.05 Å,²⁴ this value of the work function change can be shown³⁸ to be equivalent to the transfer of approximately 0.02 electron from the ruthenium surface to each oxygen adatom of the $p(2 \times 2)$ overlayer, representing a quantifiable increase in the Lewis acidity of the ruthenium surface atoms. The actual electron transfer will be somewhat greater than this estimate which ignores polarization. This increases the ability of the ruthenium surface atoms to accept lone pair electrons from adsorbates and inhibits the ability of the former to backdonate electrons to otherwise unoccupied adsorbate levels. The dramatic effect of the $p(2 \times 2)$ oxygen overlayer on the electronic structure of the Ru(001) surface has been demonstrated in previous investigations of the chemisorption of acetone³⁹ and formaldehyde.⁴⁰ Both of these molecules are π acids like N_2 and CO, and both have occupied lone pair orbitals for σ donor bonding and unoccupied antibonding orbitals of π^* symmetry for backdonor bonding to metal surfaces. Whereas the σ donor and π^* backdonor contributions to the bonds which N_2 and CO form with the Ru(001) surface can be measured only in terms of binding energies and intramolecular stretching frequencies, the balance between the strengths of the σ donor and π^* -backdonor interactions for acetone and formaldehyde with this surface is evidenced by the configurations in which they bond. For both acetone and formaldehyde, adsorption on the clean Ru(001) surface produces η^2 configurations indicative of strong π^* backdonor bonding. On the Ru(001) surface, modified by the presence of the $p(2 \times 2)$ oxygen overlayer, however, σ donor bonding in an η^1 configuration is stabilized with respect to π^* backdonor bonding for both acetone and formaldehyde.

Qualitatively similar results are apparent here for the adsorption of N_2 . The appearance of $\nu(NN)$ at 2263 cm^{-1} (higher than is observed under any conditions for the adsorption of N_2 on the clean surface) for N_2 adsorbed on the Ru(001) surface on which a $p(2 \times 2)$ oxygen overlayer is present indicates that the oxygen decreases the already weak $1\pi_g$ backdonation contribution to the Ru- N_2 bond. Even with decreased backdonation, however, the binding energy of the N_2 molecules to the ruthenium surface is increased. This implies that for N_2 on the clean Ru(001) surface, $1\pi_g$ backdonation contributes little to the Ru- N_2 bond strength. It is the increased strength of the dominant σ donation contribution to the bonding which is evidenced in the TDMS results for the $p(2 \times 2)$ oxygen precovered surface, and this effect is specific to N_2 molecules that are adsorbed within the $p(2 \times 2)$ overlayer of oxygen adatoms.

An interesting comparison of these results to those of a previous investigation of oxygen and CO coadsorption on the Ru(001) surface¹⁸ can be drawn. The effects of preadsorbed, ordered oxygen on the EEL spectrum of subsequently adsorbed CO are similar to those reported here: $\nu(CO)$ increased to 2032 cm^{-1} from 1990 cm^{-1} on the clean surface, indicating decreased 2π backdonor bonding in the pres-

ence of oxygen. The thermal desorption results, however, indicated a decrease of the Ru-CO binding energy by approximately 6 kcal/mol in the presence of ordered oxygen. Moreover, in agreement with the results reported here, a more recent investigation has shown that this effect for CO on Ru(001) depends critically on the oxygen overlayer being ordered prior to exposure of the surface to CO.¹⁹ This result confirms, as expected, that the 2π backdonor contribution to the Ru-CO bond contributes significantly to the binding energy of CO on the Ru(001) surface, much more so than $1\pi_g$ backdonor bonding for N_2 .

C. Adsorption of carbon monoxide on the Ru(001) surface precovered with overlayers of nitrogen

Thermal desorption spectra recorded after exposure of the clean Ru(001) surface to 2.25 L of N_2 at 75 K, an exposure that produces a fractional surface coverage of 0.44, followed by increasing exposures to CO at 75 K are shown in Fig. 10. For fractional surface coverages of CO below approximately 0.22, the adsorbed N_2 in both apparent binding states which are present on the clean surface is readily displaced by CO, as would be expected based on a comparison of their binding energies to the Ru(001) surface. The probability of adsorption of CO on this Ru(001) surface precovered with N_2 is constant within experimental uncertainty up to this coverage and is decreased by no more than 5% compared to the value obtained for the adsorption of CO on the clean Ru(001) surface at this temperature, suggesting a similar precursor mechanism controls the rate of CO adsorption on both surfaces.¹³ For coverages of CO equal to or greater than approximately 0.22 monolayer, the attenuation of the high temperature state exceeds that of the low temperature state of N_2 . For coverages approaching 0.5 monolayer of CO, desorption of the remaining N_2 occurs only in the low temperature peak near 90 K. It is important to note that as CO is added to and N_2 displaced from the Ru(001) surface in the measurements of Fig. 10, the total fractional

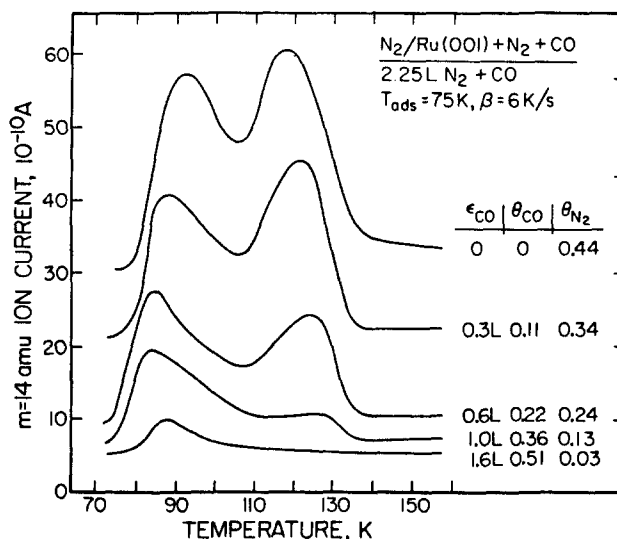


FIG. 10. Thermal desorption spectra of N_2 recorded after the indicated exposures of CO at 75 K to the Ru(001) surface, preexposed to 2.25 L of N_2 at 75 K.

surface coverage of both species remains nearly constant at a value between 0.44 and 0.54. This suggests that the effective surface area of each added CO molecule is nearly equal to that of the N_2 molecule which it displaces.

These observations, considered in conjunction with the results of previous investigations which have described the behavior of adsorbed CO on the clean Ru(001) surface,^{22,37,41} allow a reasonable mechanism for the desorption of N_2 in the presence of coadsorbed CO to be developed, which explains the effects evident in Fig. 10. On the clean Ru(001) surface, attractive lateral interactions on the order of 0.75 kcal/mol at the $\sqrt{3}$ intermolecular spacing of 4.66 Å lead to the formation of islands of the $(\sqrt{3} \times \sqrt{3})R30^\circ$ structure at coverages of CO below 0.33 monolayer.⁴¹ As the coverage of CO is increased beyond 0.33 monolayer, repulsive lateral interactions produce uniform two-dimensional compression of the CO overlayer, causing the CO ad molecules to lose registry with the on-top adsorption sites which are occupied at low coverage. Commensurate hexagonal overlayers which result from this compression are observed at fractional surface coverages of $7/12 [(\sqrt{3} \times \sqrt{3})R30^\circ]$ and $49/75 [(5\sqrt{3} \times 5\sqrt{3})R30^\circ]$.²² On the basis of a kinetic model for the rate of CO desorption from the clean Ru(001) surface, the pairwise repulsion which leads to compression of the CO overlayer for fractional surface coverages in excess of 0.33 has been estimated to be approximately 3 kcal/mol.⁴¹ The results of the EELS measurements, to be discussed below, suggest that as CO is added to the Ru(001) surface precovered with a saturated overlayer of N_2 , segregation of the CO ad molecules into islands begins as the coverage of CO exceeds approximately 0.10 monolayer. Since the total surface coverage of N_2 and CO remains nearly constant at approximately 0.5 monolayer as CO is added, the islands of CO are compressed to a surface density greater than that of the optimal $(\sqrt{3} \times \sqrt{3})R30^\circ$ overlayer by the presence of the coadsorbed N_2 . Throughout the CO coverage range, the N_2 molecules remaining in the areas between and around the CO islands maintain the surface density typical for the adsorption of N_2 on the clean surface at 75 K. As the desorption of N_2 proceeds, expansion of the islands of CO maintains additional N_2 molecules in the crowded binding sites associated with the low temperature desorption peak. This explains the more rapid attenuation of the high temperature state compared to the low temperature state of N_2 for coverages of CO equal to or greater than 0.22, and the lack of significant desorption from the high temperature state of N_2 for coverages of CO in excess of 0.33 monolayer in the thermal desorption spectra of Fig. 10.

The results of an experiment designed to test this hypothesis are shown in Fig. 11. The spectrum at the top of Fig. 11 shows desorption of N_2 from a partially filled $(\sqrt{3} \times \sqrt{3})R30^\circ$ overlayer, formed by exposing the clean Ru(001) surface to 2.25 L of N_2 at 100 K. The resulting surface coverage is 0.22 monolayer, and the low temperature "binding state" for N_2 is left unpopulated. For the spectrum at the bottom of Fig. 11, an identically prepared overlayer of N_2 was exposed to 1.0 L of CO at 75 K, producing a coverage of CO of 0.39 monolayer and reducing the coverage of N_2 to

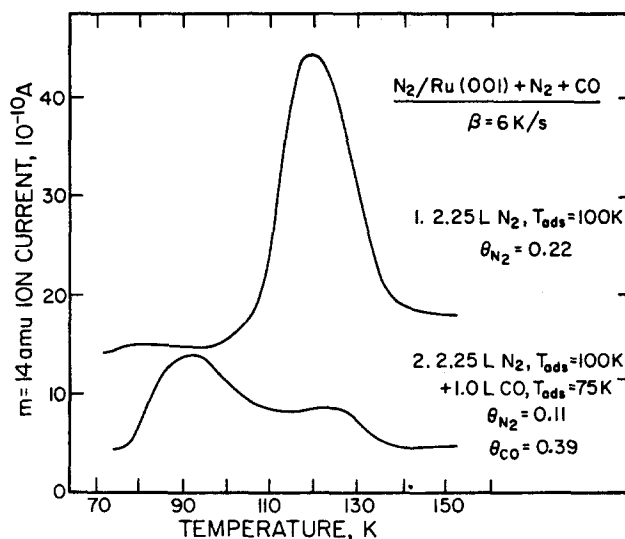


FIG. 11. Thermal desorption spectra of N_2 illustrating both the displacement and the shift to sites of lower binding energy of adsorbed N_2 by subsequently adsorbed CO. Spectrum (1), for exposure of the clean Ru(001) surface to 2.25 L N_2 at 100 K, shows the occupation of the state associated with the $(\sqrt{3} \times \sqrt{3})R30^\circ$ overlayer of N_2 . Spectrum (2) shows the desorption of N_2 from an overlayer prepared via the same procedure as for (1), and then exposed to 1.0 L CO at 75 K.

0.11 monolayer. The resulting desorption spectrum for N_2 is nearly identical to that shown in Fig. 10 for a 1.0 L exposure of CO and demonstrates clearly the shift of N_2 ad molecules from the high energy to the low energy binding sites upon the adsorption of CO.

Electron energy loss spectra recorded after exposure of the clean Ru(001) surface to 4 L of N_2 at 85 K, an exposure sufficient to produce a fractional surface coverage of 0.40 monolayer, followed by the indicated exposures to CO, are shown in Fig. 12. Several important features of these spectra should be noted. First, the anomalously low value of $\nu(\text{CO})$ observed in the bottom spectrum, 1958 cm^{-1} , is evidence of a perturbation of the vibrational spectrum of adsorbed CO by the presence of neighboring N_2 molecules at low coverages of CO. Furthermore, for all coverages of CO, the values of $\nu(\text{Ru-N}_2)$ ranged between 283 and 295 cm^{-1} , and the values of $\nu(\text{NN})$ ranged between 2197 and 2216 cm^{-1} . These values are typical of high coverages of N_2 on the clean surface (cf. Fig. 5) and suggest that the N_2 molecules are segregated from the CO molecules as the CO surface coverage is increased. Finally, the peak at 247 cm^{-1} in the spectrum at the top of Fig. 12 is not due to adsorbed N_2 , but rather results from a surface phonon which couples to the hexagonal compression structure that CO forms on the clean Ru(001) surface for coverages near 0.5 monolayer. Thermal desorption measurements indicate that approximately 0.02 monolayer of N_2 is present on the surface for this spectrum, but the features due to adsorbed N_2 are too weak for this coverage of N_2 to be resolved from the strong modes due to adsorbed CO.

Figure 13 shows the frequency of $\nu(\text{CO})$ as a function of the coverage of CO for experiments performed under conditions identical to those represented by the EEL spectra of Fig. 12. For comparison, the frequency of $\nu(\text{CO})$ is shown as a function of the coverage of CO for adsorption on the clean

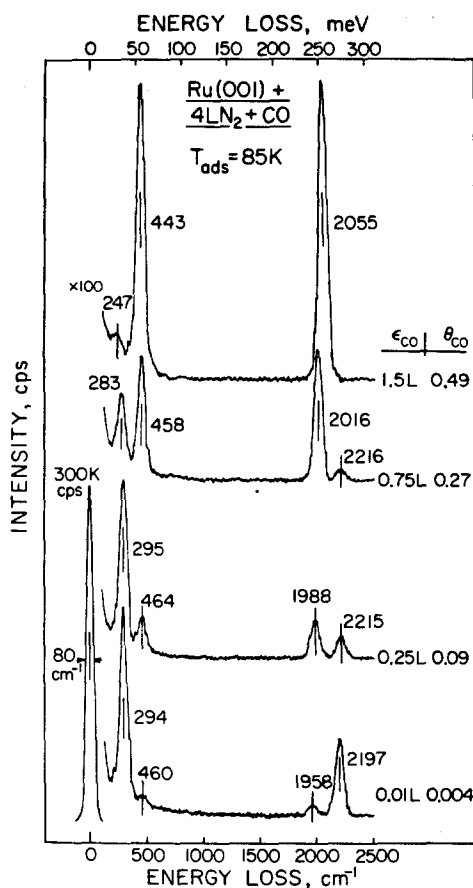


FIG. 12. EEL spectra recorded after exposure of the clean Ru(001) surface to 4 L N₂ at 85 K, followed by the indicated exposures to CO at 85 K.

Ru(001) surface. The lines drawn through the data points in this figure are merely a visual guide. Several important effects are evident in these data. First $\nu(\text{CO})$ at low coverage on the N₂ precovered surface is 34 cm⁻¹ lower than the lowest value of $\nu(\text{CO})$ observed on the clean surface. In addition, $\nu(\text{CO})$ increases sharply from this low value until a coverage of CO of approximately 0.10 monolayer is reached, indicating that changes which strongly affect the

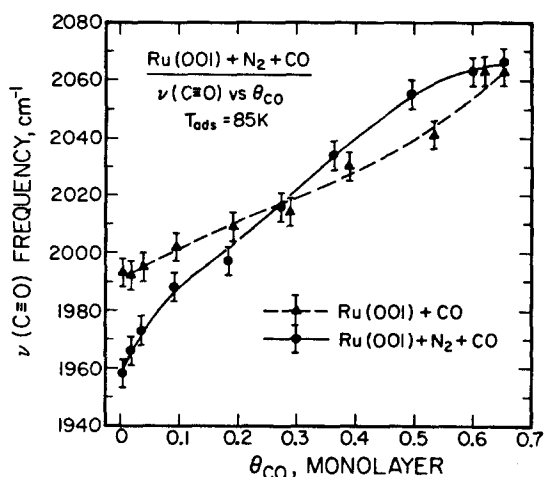


FIG. 13. The frequency of $\nu(\text{CO})$ as a function of the fractional surface coverage of CO for adsorption on both the clean and on the Ru(001) surface precovered by a 4 L exposure to N₂ at 85 K.

vibrational structure of the mixed overlayer are occurring in this coverage range. Finally, the curve for CO adsorption on the N₂ precovered surface crosses the curve for CO adsorption on the clean surface at a coverage of CO near 0.3 monolayer. As will be discussed below, all of these results are consistent with CO island formation which causes CO and N₂ to be segregated into different local areas of the surface for CO coverages greater than approximately 0.10 monolayer.

The first evidence which supports this conclusion is the nearly constant value of $\nu(\text{NN})$ that is observed as the CO coverage is varied. In the limit of infinite dilution of N₂ in an overlayer of CO (i.e., a single N₂ molecule as an interstitial impurity in an overlayer of CO), the effect of dipolar interactions with the surrounding CO ad molecules on $\nu(\text{NN})$ is described by the solution of

$$\left(\frac{\omega}{\omega_0}\right)^2 = 1 + \frac{\alpha_v \Sigma}{1 + \alpha_e \Sigma},$$

where ω_0 is the zero coverage value of $\nu(\text{NN})$, but α_v , α_e , and Σ are appropriate to the CO overlayer.⁶ Consequently, N₂ molecules that are surrounded by CO molecules have $\nu(\text{NN})$ blue shifted by dipolar interactions with the CO molecules, just as a CO molecule would in the same environment. For a single N₂ molecule in a ($\sqrt{3} \times \sqrt{3}$)R30° overlayer of CO, $\nu(\text{NN})$ would increase from its zero coverage value of 2247 to 2283 cm⁻¹, in the absence of other interactions which affect $\nu(\text{NN})$. The only other interaction which would contribute to a significant change in $\nu(\text{NN})$ is competition for electron density to be donated into the 2 π antibonding orbital of the CO ad molecules and the 1 π_g antibonding orbital of the N₂ ad molecules. As was discussed earlier and demonstrated with the results for the coadsorption of N₂ with oxygen, N₂ is a weaker π acid than CO. Thus N₂ should lose 1 π_g electron density in the presence of CO, further increasing $\nu(\text{NN})$. The low values of $\nu(\text{NN})$ observed in the presence of coadsorbed CO are only consistent with N₂ molecules adsorbed in areas of the surface that are free of CO, where their behavior mimics that observed for the adsorption of N₂ on the clean Ru(001) surface.

The value of $\nu(\text{CO})$ observed for a low coverage of CO in the presence of N₂, 1958 cm⁻¹, has important consequences for understanding the bonding of N₂ to the clean Ru(001) surface. Results of an infrared reflection-absorption spectroscopic investigation of the chemisorption of CO on Ru(001),⁴² as well as the EELS data for the adsorption of CO on the clean surface presented in Fig. 13, demonstrate clearly that $\nu(\text{CO})$ in the limit of zero coverage on Ru(001) is approximately 1990 cm⁻¹. Employing the analysis presented above, the value of $\nu(\text{CO})$ expected for a single CO ad molecule surrounded by N₂ molecules is approximately 2002 cm⁻¹. Thus, the low value of $\nu(\text{CO})$ observed in the presence of a "sea" of N₂ is clearly the result of changes in the Ru-CO bond produced by the adsorption of N₂. From this effect, manifest in the vibrational spectrum of a small concentration of CO coadsorbed with N₂, it can be inferred that the decrease of $\nu(\text{NN})$ with increasing surface coverage of N₂ on the clean surface cannot be due simply to the formation of a 1 π_g band with increasing surface coverage; the increasing dispersion of which increases its population and

causes $\nu(\text{NN})$ to decrease.³⁴ If $1\pi_g$ band formation were the dominant mechanism, the 2π antibonding orbital of the CO added to the surface on which a high coverage of N_2 is present would not participate in the $1\pi_g$ band, but would rather compete with N_2 for the electron density available at the surface for backdonation. The value of $\nu(\text{CO})$ observed in this circumstance would reflect this competition for electron density and would be expected to be similar to that observed for CO adsorption on the clean Ru(001) surface, modified only by the presence of dipolar interactions with the N_2 admolecules which surround the adsorbed CO. Instead, the low value of $\nu(\text{CO})$ observed under these circumstances indicates that the ruthenium surface atoms have their Lewis basicity, as measured by their ability to backdonate electrons into the $1\pi_g$ orbital of adsorbed N_2 or the 2π orbital of adsorbed CO, increased by the presence of N_2 on the surface. *This implies that a mechanism for the decrease of $\nu(\text{NN})$ with increasing surface coverage of N_2 on the Ru(001) surface which considers only $1\pi_g$ band formation in the adsorbate overlayer is inadequate.*

The strong shift of $\nu(\text{CO})$ with increasing coverage, observed for coverages of CO between zero and 0.10 monolayer, indicates that significant changes in the environment of the CO admolecules occur in this coverage range. A part of this frequency shift can be attributed to the decreasing coverage of N_2 on the surface as the CO is added, increasing $\nu(\text{CO})$ through the mechanism described in the preceding paragraph. This effect alone, however, would be expected to give a more gradual increase of $\nu(\text{CO})$ between zero coverage and the coverage of CO at which no N_2 remains on the surface (approximately 0.6 monolayer, cf. Fig. 13). Two other effects contribute additively to give the observed sharp increase of $\nu(\text{CO})$, both of which must be attributed to the segregation of CO admolecules into islands as the coverage of CO increases. One mechanism is the increased dipolar coupling of CO, which exists with near neighbor CO admolecules compared with near neighbor N_2 admolecules, due to the high value of the vibrational polarizability of CO ($\alpha_v = 0.28 \text{ \AA}^3$)⁶ relative to that of N_2 ($\alpha_v = 0.09 \text{ \AA}^3$). Furthermore, the segregation of CO admolecules into islands would reduce the *local* effect of coadsorbed N_2 on the backdonor properties of the ruthenium atoms to which the CO molecules bind, producing a sharp upward shift of $\nu(\text{CO})$ as the occupation of the 2π orbitals of CO is decreased in this coverage range. If island formation did not occur, but rather a homogeneous mixed overlayer of N_2 and CO existed at all coverages of CO, these two effects would be distributed over a broader range of CO coverages, and a more uniform increase of $\nu(\text{CO})$ with coverage would result.

Finally, the increase of $\nu(\text{CO})$, evident in Fig. 13 for coverages above 0.3 monolayer in the presence of coadsorbed N_2 , to values greater than that observed for the same coverage of CO on the clean Ru(001) surface gives a further indication of the compression of adsorbed CO by the N_2 in this coverage range. Notice in the data of Fig. 13 that $\nu(\text{CO})$, for a coverage of CO of approximately 0.4 monolayer in the presence of N_2 matches that observed for CO alone on the surface at a coverage near 0.5 monolayer. This indicates that the CO admolecules in both of these circum-

stances are in the same environment, i.e., the local surface density (CO molecules per ruthenium surface atom) is the same in both cases. This corresponds well with the TDMS results of Fig. 10, where it was demonstrated that the total surface coverage, and therefore the local surface density of each species, remains nearly constant as the CO coverage is increased and N_2 molecules are displaced from the coadsorbed overlayer.

IV. SUMMARY

The principal results of this work may be summarized as follows:

(1) Due to a local perturbation of the electronic structure of the Ru(001) surface, the $p(2 \times 2)$ ordered overlayer of oxygen adatoms increases the σ donor contribution and decreases the $1\pi_g$ backdonor contribution to the bond which N_2 forms with this surface. The net increase in the binding energy of N_2 to the Ru(001) surface is approximately 1.5 kcal/mol. These results are qualitatively different from those obtained for the coadsorption of CO with oxygen, where a decrease in the binding energy of CO was observed in the presence of oxygen. This indicates that backdonor bonding contributes more significantly to the bond which CO forms than that which N_2 forms with the Ru(001) surface.

(2) The results of measurements for the adsorption of CO on the Ru(001) surface precovered with a saturated monolayer of N_2 are consistent with CO island formation and segregation of the two species into different local regions on the surface for CO coverages above 0.10 monolayer. An anomalously low value of $\nu(\text{CO})$ is observed for low coverages of CO surrounded by N_2 on the surface, giving clear evidence of a modification in the local electronic properties of the Ru(001) surface by chemisorbed N_2 . The N_2 admolecules increase the ability of the ruthenium surface atoms to backdonate electron density to the π^* antibonding orbitals of π acid molecules like CO, and this effect also explains the coverage-dependent decrease of $\nu(\text{NN})$ observed for the adsorption of N_2 on the clean Ru(001) surface.

(3) The details of the interaction of a single adsorbed species with a clean metal surface, in this case N_2 with Ru(001), can be clarified by carefully designed experiments which feature coadsorption with other species, the adsorption characteristics of which are well understood. In this case, a clearer picture of the bonding of N_2 to the Ru(001) surface has emerged from experiments with coadsorbed oxygen and CO.

ACKNOWLEDGMENT

This research was supported by the National Science Foundation under Grant No. CHE-8516615.

APPENDIX

The EELS results obtained for the adsorption of N_2 on the clean Ru(001) surface at 95 K show $\nu(\text{NN})$ appearing initially at 2252 cm^{-1} and shifting to 2212 cm^{-1} at a saturation coverage of 0.33 monolayer, where a $(\sqrt{3} \times \sqrt{3})\text{R}30^\circ$ superstructure is formed. An estimate of the contribution of

dipolar vibrational coupling to the coverage dependence of $\nu(\text{NN})$ can be made by using the following information:

(1) The intensity of the $\nu(\text{NN})$ feature for a saturation coverage of N_2 at 95 K, where a $(\sqrt{3} \times \sqrt{3})\text{R}30^\circ$ overlayer is formed, is approximately one-third of that observed for the same overlayer of CO on the Ru(001) surface (with the same incident electron kinetic energy and electron analyzer acceptance angle). For the latter, accurate values of the vibrational polarizability α_v , the electronic polarizability α_e , and the dipole lattice sum Σ have been obtained.⁶

(2) Since the bond lengths of adsorbed N_2 and CO are certainly equal to within less than 0.2 \AA ,^{8,10} the dipole lattice sums for $(\sqrt{3} \times \sqrt{3})\text{R}30^\circ$ overlayers of N_2 and CO can be assumed to be equal, i.e., $\Sigma = 0.17 \text{ \AA}^{-3}$.

(3) Applications of this theory to other adsorption systems has shown that although α_v may differ significantly from its gas phase value for an adsorbed molecule, α_e is nearly unchanged upon chemisorption.^{4,43} Consequently, the gas phase value of α_e , 2.4 \AA^3 ,⁴⁴ can be used as a good approximation in this analysis.

Employing these approximations and the results obtained for the analysis of CO on Ru(001), a value of $\alpha_v = 0.09 \text{ \AA}^3$ is calculated with an estimated accuracy of $\pm 20\%$ for adsorbed N_2 on Ru(001). Note that this result follows from the use of the cross section for dipolar inelastic scattering from the $\nu(\text{NN})$ vibration at a single coverage. Inserting the frequency for $\nu(\text{NN})$ observed for low coverages of N_2 on the Ru(001) surface, $\omega_0 = 2252 \text{ cm}^{-1}$, the calculated value of $\alpha_v = 0.09 \text{ \AA}^3$, and the assumed values of $\alpha_e = 2.4 \text{ \AA}^3$ and $\Sigma = 0.17 \text{ \AA}^{-3}$ into the expression for the frequency shift due to dipolar coupling upon going from a surface coverage of zero to the $(\sqrt{3} \times \sqrt{3})\text{R}30^\circ$ overlayer, given in Sec. III C, yields $\omega = 2264 \text{ cm}^{-1}$ at $\theta = 0.33$ for N_2 on Ru(001), an increase of approximately 12 cm^{-1} . Variation of α_e by $\pm 50\%$ from its gas phase value of 2.4 \AA^3 only changes this result by $\pm 1 \text{ cm}^{-1}$. Since the experimental results for N_2 show a net decrease of 40 cm^{-1} when going from $\theta = 0$ to $\theta = 0.33$, and the previous analysis shows that an increase of 12 cm^{-1} occurs due to dipolar coupling, it follows that a decrease of approximately 52 cm^{-1} in $\nu(\text{NN})$ occurs due to coverage-dependent chemical changes in the $\text{N} \equiv \text{N}$ bond.

¹K. Hermann and P. S. Bagus, Phys. Rev. B **16**, 4195 (1977).

²A. Rosen, P. Grundevik, and T. Morovic, Surf. Sci. **95**, 477 (1980).

³J. Paul and A. Rosen, Phys. Rev. B **26**, 4073 (1982).

⁴H. Ibach and D. L. Mills, *Electron Energy Loss Spectroscopy and Surface Vibrations* (Academic, New York, 1982).

⁵B. E. Nieuwenhuys, Surf. Sci. **105**, 505 (1981).

⁶B. N. J. Persson and R. Ryberg, Phys. Rev. B **24**, 6954 (1981).

⁷K. Hermann, P. S. Bagus, C. R. Brundle, and D. Menzel, Phys. Rev. B **24**, 7025 (1981).

⁸A. Schichl, D. Menzel, and N. Rösch, Chem. Phys. Lett. **65**, 225 (1982).

⁹A. Schichl, D. Menzel, and N. Rösch, Chem. Phys. Lett. **105**, 285 (1984).

¹⁰C. W. Bauschlicher, Chem. Phys. Lett. **115**, 387 (1985).

¹¹C. R. Brundle, P. S. Bagus, D. Menzel, and K. Hermann, Phys. Rev. B **24**, 7041 (1981).

¹²J. Stöhr and R. Jaeger, Phys. Rev. B **26**, 4111 (1982).

¹³D. Menzel, H. Pfnür, and P. Feulner, Surf. Sci. **126**, 374 (1983).

¹⁴K. Horn, J. DiNardo, W. Eberhardt, H.-J. Freund, and E. W. Plummer, Surf. Sci. **118**, 465 (1982).

¹⁵An estimate of this energy difference can be obtained by comparing the energies of the shape resonances associated with temporary occupation of these orbitals in gas phase electron impact scattering experiments. The 2π -derived shape resonance of CO appears at 1.7 eV, 0.6 eV lower than the corresponding $1\pi_g$ -derived shape resonance of N_2 . See G. J. Schultz, Rev. Mod. Phys. **45**, 423 (1973).

¹⁶J. L. Gland, R. J. Madix, R. W. McCabe, and C. DeMaggio, Surf. Sci. **143**, 46 (1984).

¹⁷F. M. Hoffmann and R. A. de Paola, Phys. Rev. Lett. **52**, 1697 (1984).

¹⁸G. E. Thomas and W. H. Weinberg, J. Chem. Phys. **70**, 954 (1979).

¹⁹H.-I. Lee, G. Praline, and J. M. White, Surf. Sci. **91**, 581 (1980).

²⁰Preliminary results have been published for N_2 on Ru(001); see A. B. Anton, N. R. Avery, B. H. Toby, and W. H. Weinberg, J. Electron Spectrosc. **29**, 181 (1983).

²¹G. E. Thomas and W. H. Weinberg, Rev. Sci. Instrum. **50**, 497 (1979).

²²E. D. Williams and W. H. Weinberg, Surf. Sci. **82**, 93 (1979).

²³P. Feulner and D. Menzel, Phys. Rev. B **25**, 4295 (1982).

²⁴T. S. Rahman, A. B. Anton, N. R. Avery, and W. H. Weinberg, Phys. Rev. Lett. **51**, 1979 (1983).

²⁵T. E. Madey, H. A. Engelhardt, and D. Menzel, Surf. Sci. **48**, 304 (1975).

²⁶P. A. Redhead, Vacuum **12**, 203 (1962).

²⁷Theoretical simulations suggest that the inherent (low coverage) binding energy of N_2 on Ru(001) is 5.8 kcal/mol, with an additional attractive interaction energy of 1.4 kcal/mol when the N_2 is adsorbed in a $(\sqrt{3} \times \sqrt{3})\text{R}30^\circ$ superstructure (Ref. 28).

²⁸E. S. Hood, B. H. Toby, and W. H. Weinberg, Phys. Rev. Lett. **55**, 2437 (1985).

²⁹M. M. Hills and W. H. Weinberg (unpublished results).

³⁰B. Folkesson, Acta Chem. Scand. **26**, 4008 (1972).

³¹P. Hollins and J. Pritchard, Surf. Sci. **89**, 486 (1979).

³²M. L. Kottke, R. G. Greenler, and H. C. Tompkins, Surf. Sci. **32**, 231 (1972).

³³M. Grunze, R. K. Driscoll, G. N. Burland, J. C. L. Cornish, and J. Pritchard, Surf. Sci. **89**, 381 (1979).

³⁴D. P. Woodruff, B. E. Hayden, K. Prince, and A. M. Bradshaw, Surf. Sci. **123**, 397 (1982).

³⁵C. F. McConville, C. Somerton, and D. P. Woodruff, Surf. Sci. **139**, 75 (1984).

³⁶J. Rogozik, H. Scheidt, V. Dose, K. C. Prince, and A. M. Bradshaw, Surf. Sci. **145**, L481 (1984).

³⁷E. D. Williams, W. H. Weinberg, and A. C. Sobrero, J. Chem. Phys. **76**, 1150 (1982).

³⁸J. Topping, Proc. R. Soc. London Ser. A **114**, 67 (1927).

³⁹N. R. Avery, W. H. Weinberg, A. B. Anton, and B. H. Toby, Phys. Rev. Lett. **51**, 682 (1983); A. B. Anton, N. R. Avery, B. H. Toby, and W. H. Weinberg, J. Am. Chem. Soc. **108**, 684 (1986).

⁴⁰A. B. Anton, J. E. Parmeter, and W. H. Weinberg, J. Am. Chem. Soc. **107**, 5558 (1985); (in press).

⁴¹H. Pfnür, P. Feulner, H. A. Engelhardt, and D. Menzel, Chem. Phys. Lett. **59**, 481 (1978).

⁴²H. Pfnür, D. Menzel, F. M. Hoffmann, A. Orgeta, and A. M. Bradshaw, Surf. Sci. **93**, 431 (1980).

⁴³B. N. J. Persson and A. Liebsch, Surf. Sci. **110**, 356 (1981).

⁴⁴K. L. Wolf, H. Briegleb, and H. A. Stuart, Z. Phys. Chem. B **6**, 429 (1929).